Zinc Oxide and IGZO Bi-layer Synaptic Device with Highly Linear Long-term Potentiation and Depression Characteristics

Hyun-Woong Choi
Chungnam National University
Ki-Woo Song
Chungnam National University
Seong-Hyun Kim
Chungnam National University
Nguyen Kim Thanh
Chungnam National University
Sunil Babu Eadi
Chungnam National University
Hyuk-Min Kwon
Semiconductor Convergence Campus of Korea Polytechnic College
Hi-Deok Lee (hdlee@cnu.ac.kr)
Chungnam National University

Research Article

Keywords: Potentiation Characteristics, Depression Characteristics, neuromorphic

Posted Date: August 26th, 2021

DOI: https://doi.org/10.21203/rs.3.rs-835526/v1

Abstract

The electrical properties, resistive switching behavior, and long-term potentiation/depression (LTP/LTD) in a single indium-gallium-zinc-oxide (IGZO) and bi-layer IGZO/ZnO memristors were investigated for synapse application. The use of oxide bi-layer memristor, in particular, improved electrical properties such as stability, reliability of memristors, and increase in the synaptic weight states. Bi-layer IGZO/ZnO memristors had a set voltage of 0.9 V, and reset voltage around -0.7 V, resulting in low-power consumption for neuromorphic systems. The oxygen vacancies in X-ray photoelectron spectroscopy analysis played a role in the modulation of the high-resistance state (HRS) (oxygen-deficient) and the low-resistance state (oxygen-rich) region. The V_{RESET} of bi-layer IGZO/ZnO memristors was lower than that of a single IGZO, which implied that oxygen vacancy filaments could be easily ruptured due to the higher oxygen vacancy peak HRS layer. The nonlinearity of LTP and LTD characteristics in a bi-layer IGZO/ZnO memristor was 6.77% and 11.49%, respectively, compared to those of 20.03% and 51.1% in a single IGZO memristor, respectively. Therefore, the extra ZnO layer in the bi-layer memristor with IGZO was potentially significant and essential to achieve a small set voltage and a reset voltage, and the switching behavior to form the conductive path.

Introduction

In complex situations, the human brain can process information in parallel and accurately recognize objects and visual information[1,2]. Neuromorphic information processing systems have been expected to be the next-generation computing technology that will be able to transcend the limitations of conventional information processing systems like Von Neumann Computing. The use of memory structures is the most significant difference between neuromorphic systems and conventional information processing systems. In conventional information processing systems, several transistors and capacitors have been used to emulate a single synapse, increase power consumption, and limit the density of integration[3–5]. Many kinds of research are currently studied to develop a single device with a new concept that simultaneously performs inherent learning and data storage functions without memory devices[6–11]. Recently, resistive switching random access memory (ReRAM) is considered to be the most promising candidate for synaptic devices due to their capability of conductance modulation. Also, ReRAM with a metal-insulator-metal structure capable of realizing synaptic networks has an advantage of integration at high density ($4F^2$) due to the simple structure, fast-switching speed, lower power consumption, and higher scalability[12–14].

Among the various dielectric materials used as resistive switching (RS) layers, such as hafnium oxide[15,16], tantalum oxide[17,18] and titanium oxide[19–21], indium-gallium-zinc-oxide (IGZO) and zinc oxide (ZnO) have attracted much attention as one of the most promising due to its outstanding good uniformity for large area deposition, low cost, and multiple functions abilities[22,23]. Furthermore, an advantage of IGZO material is an easy switching of the RS behavior as the mobility of the carrier increased due to the increase in indium concentration, which enables a high-speed operation. Following a

high driving current, the amount of oxygen vacancy in the IGZO layer has been controlled by gallium concentration[24,25]. ZnO is an excellent material of chemical stability, a wide direct bandgap, and high transparency properties. However, because the donor defects in ZnO materials contribute to n-type conduction, it is difficult to achieve high resistive ZnO switching films. The high-resistance state (HRS) layer is placed at the top of the bi-layer structure, which results in good switching behavior. However, the linear and symmetric changes in conductance with the number of potentiation and depression pulses should be important to memristor devices for hardware-based neural networks. Single-layer memristor devices' potentiation and depression characteristics are often nonlinear, resulting in less efficient neural network processing. In particular, it is believed that the structure of the bi-layer memristor device achieves high linearity of the potentiation and depression characteristics. However, the electrical properties of the ReRAM with an additional oxide layer between the bottom electrode and the IGZO layers are yet to be studied. The use of oxide bi-layers showed improvement in electrical properties such as stability, reliability of memristors, and increase in the synaptic weight states.[26–28].

This paper proposed bi-layer IGZO/ZnO memristors to improve the electrical characteristics and synaptic linearity in long-term potentiation/depression (LTP/LTD) characteristics compared with a single IGZO memristors. The role of the potential barrier between the bottom electrode and HRS material was verified to the conduction mechanism of charge transport behavior at HRS and low-resistance state (LRS). In particular, the high linearity in LTP/LTD characteristics of bi-layer IGZO/ZnO memristors shows more linear than that of other reported devices to our knowledge[29–32].

Experiments

A single structure of memristor crossbar was fabricated to a square type, as shown in Fig. 1, which could be integrated at high density. The Ti layer as the bottom electrode was deposited by 100 nm using a radio frequency (RF) sputtering system and patterned by the lift off process with photolithography. There are two types of memristors; one is a single IGZO memristor, and the other is a bi-layer IGZO/ZnO memristor. The single layer IGZO was deposited by using the RF sputtering system as follows. First, 50 nm-thick IGZO used as an HRS was deposited with the molecular composition of In:Ga:Zn = 1:1:1 at a working pressure of 2 mTorr (Ar gas flow rate: 30 standard cubic centimeters per min (sccm)) without substrate heating (substrate temperature < 50 ℃). Then, the 10 nm-thick IGZO for an LRS was deposited with the molecular composition of In:Ga:Zn = 2:2:7, and other conditions were same above. When IGZO layers for HRS and LRS were deposited, the oxygen gas flow was adjusted as 20 sccm and 1 sccm, respectively, to control the amount of oxygen vacancy. For the bi-layer IGZO/ZnO structure, 50 nm ZnO layer was deposited by atomic layer deposition system using DEZn (diethylzinc, $Zn(CH_2CH_3)_2$) and an H_2O of source precursors at a chamber temperature of 80 ℃, and followed by the deposition of 10 nm IGZO as an LRS using RF sputtering system. Finally, the Ti layer was deposited as the top electrode using the RF sputtering system, which is identical to the bottom electrode process through photolithographic patterning to form a crossbar type device. Figure 1(b) showed the top-view scanning electron microscopy (SEM) images of 20 μm × 20 μm crossbar structure.

At room temperature, the electrical properties across a single IGZO and bi-layer IGZO/ZnO memristors were measured using the Keysight B1500A semiconductor device analyzer. The current compliance was applied for the transition from HRS to LRS. The voltage pulses across a single IGZO and bi-layer IGZO/ZnO memristors were applied by the Keysight B1530 waveform generator/fast measurement unit which also has the current and voltage measurement functions. Precision and long-term sampling measurements were used to measure the current across the diffusive memristor and to measure the voltage at the output of the waveform generator. The long-term sampling measurements allowed the application of pulse signals down to 100 ns and precise current measurement at a sampling rate of 50 ns. The write pulse with amplitude (3 V) across a single IGZO and bi-layer IGZO/ZnO memristors was applied, and then a short duration (20 or 50 ms) was used as the read voltage to minimize disturbance on device conductance. The applied positive/negative pulses were 50 for single IGZOs and 100 for bi-layer IGZO/ZnO memristors, respectively, and the current was measured after each stimulation pulse was applied. All equipment in the setup is controlled by the Agilent Easy Expert software.

Results And Discussion

Figure 2 shows the RS behaviors of ten cycles in a single IGZO and bi-layer IGZO/ZnO memristors. This result shows the typical bipolar RS characteristics with the bottom electrode grounded in electrical measurements. The memristor devices are initially in HRS state. With a compliance current of 1 mA, a voltage sweep is applied to the top electrode from 0 to 2 V (meaning arrow “1” in the figure), and the RS behaviors of a single IGZO and bi-layer IGZO/ZnO memristors change from the HRS to the LRS. The compliance current is set to prevent the memristor devices from being permanently damaged by a sudden increase in current levels. Once again, the voltage sweep is applied from 2 to 0 V (meaning arrow “2” in the figure) to measure the current and the RS behaviors of a single IGZO and bi-layer IGZO/ZnO memristors remain in the LRS and show a high current level. The arrows “1” and “2” in the figure are called “SET process,” which means that the RS behaviors of a single IGZO and bi-layer IGZO/ZnO memristors change from HRS to LRS. Contrary to the SET process, the process of changing from arrow “3” to “4” in the figure is called “the RESET process,” which means that the RS behaviors of a single IGZO and bi-layer IGZO/ZnO memristor changes from LRS (arrow “3”) to HRS (arrow “4”). These results can benefit the binarized neural networks (BNNs) because the conductance values (inverse of resistance value) are used as synaptic weights. The set voltages of a single IGZO and bi-layer IGZO/ZnO memristors are 1 V and 0.9 V, respectively. In contrast, the reset voltages of a single IGZO and bi-layer IGZO/ZnO memristors are about -1.8 V and -0.7 V, respectively. Therefore, in the case of IGZO/ZnO structure, the memristor device can be used as a low-power application in terms of operating voltage, suggesting that power consumption can be dramatically reduced.

X-ray photoelectron spectroscopy (XPS) measurements were performed to investigate the chemical composition of a single IGZO and bi-layer IGZO/ZnO memristors, to verify the proportions of the oxygen vacancy. Figure 3 shows the XPS analysis result of the O1s spectra in the surface following the deposition of HRS and LRS layers for a single IGZO and bi-layer IGZO/ZnO memristors, respectively, with Gaussian peak fitting. For a single IGZO and bi-layer IGZO/ZnO memristors, the proportions of the oxygen

vacancy peak (O1) of HRS layer are 45.2% and 38.2%, respectively, that of LRS layer for both memristors is about 43.4%. As the ratio of Ga and Zn determines the oxygen concentration in HRS and LRS layers during IGZO sputter-deposition, the increase in the ratio of Ga and Zn increase the number of non-oxygen vacancies in the memristor devices, resulting in a lower conductivity layer. The oxygen vacancies modulate HRS layer (oxygen-rich) into LRS layer (oxygen-deficient). The V_{RESET} of bi-layer IGZO/ZnO memristors- is lower than that of a single IGZO, which implied that oxygen vacancy filaments could be easily ruptured due to lower oxygen vacancy peak HRS layer.

To verify the mechanism of the RS behaviors for a single IGZO and bi-layer IGZO/ZnO memristors, the corresponding I–V characteristics of the SET and RESET processes are plotted in Fig. 4. For a single IGZO and bi-layer IGZO/ZnO memristors, a linear fitting slope based on the experimental data is close to 1, which means the linear relationship between current and applied voltage[33]. The charges originating from the metal electrode interface are thought to be trapped by the empty trap sites of IGZO and ZnO in the HRS layer. As the electric field across memristor devices increases, the steep current for a single IGZO is followed by a quadratic term ($I \propto V^2$) with the increase of the injected charges when the conductive filaments form between two electrodes as shown Fig. 4. When the empty trap sites are gradually occupied fully, the slope of the fitting line decreases about 2, indicating that the conduction enters the trap-free space charge limited current (SCLC). It implies that the SCLC is dominant because most injected electrons contribute to the current component[34–40].

However, the slope of the fitting line at the high electric field for bi-layer IGZO/ZnO memristor is found to be 4.0, which means that the Schottky mechanism is dominant. The Schottky mechanism in the high electric field may be due to oxygen vacancies close to the metal/metal-oxide interface. The I–V characteristics in the RESET process are dominated by the Schottky and ohmic mechanism, as shown in Fig. 4. After a single IGZO and bi-layer IGZO/ZnO memristors were changed from LRS to HRS; the switching behaviors are controlled by the interface properties due to the Schottky mechanism. It is worth noting that the SCLC is the main conduction mechanism in the SET process for a single IGZO and bi-layer IGZO/ZnO memristors. We conclude the Schottky mechanism observed in a single IGZO and bi-layer IGZO/ZnO memristors at the RESET process is attributed to the interface barrier.

Figure 5 shows the long-term potentiation/depression (LTP/LTD) characteristics with applied positive/negative pulses for an amplitude of 2 V in the two memristors. The positive (2.0 V, 400 ns) or negative (−2 V, 400 ns) voltage pulses with the interval time (4.5 μs) are applied on the memristor devices, and then, the current is measured by a reading voltage pulse (0.2 V, 1 μs) after each pulse. The LTP and LTD characteristics exhibit gradual potentiation and depression characteristics in synaptic weight depending on the input spiking signal, which can be used to evaluate whether memristors can learn or not. When a potentiating input signal train consisting of positive pulses with an amplitude of 2 V is applied on the top Ti metal of the memristor synapse (pre-neuron), the synaptic weight is changed progressively in the increase of the current, which means that the oxygen vacancies are injected into the RS layer, and then this process is formed between TE and BE for potentiation. It can emulate the potential of oxygen vacancies for neuromorphic computing, which enhances the synapse weight by releasing

neurotransmitters. In contrast, when a depressing input signal train that consists of negative pulses with an amplitude of -2 V is applied on the top metal, the synaptic weight is depressed progressively, and the conductive path formed by the oxygen vacancies move away from the bottom metal, resulting in the decrease of the current. The nonlinearity for the memristor devices is quantitatively given by equation (1)

$$Nonlinearity = average\left[\left|\frac{G - G_{Linear}}{G_{Linear}}\right| \times 100\ \%\right] \quad (1)$$

where G is the change in the conductance of memristive devices (equivalently, synaptic weight), and G_{Linear} is the linear change in conductance (determining training accuracy[41]).

Figure 5 shows that the nonlinearity of LTP and LTD characteristics in the bi-layer IGZO/ZnO memristor is 6.77% and 11.49%, respectively, while these for in a single IGZO memristor is 20.03% and 51.1%, respectively[42]. The linearity and symmetric LTP and LTD characteristics for the bi-layer IGZO/ZnO memristor show more improved linearity than for a single IGZO memristor. Therefore, the high electron conductivity of the ZnO layer in the bi-layer IGZO/ZnO memristor plays an important role in charge carriers to be injected easily under a small set voltage and a reset voltage switching behavior to form the conductive path.

Conclusion

We investigated the electrical characteristics, RS behavior, and the LTP/LTD of ZnO and IGZO and bi-layer memristors for high performance synaptic device. The set and reset voltages of bi-layer IGZO/ZnO memristors are 1 V, and -0.7 V, achieving low-power consumption to realize the neuromorphic systems. The oxygen vacancies played a role in the modulation of the HRS layer (oxygen-deficient) and the LRS layer (oxygen-rich) region. The V_{RESET} of bi-layer IGZO/ZnO memristors was lower than that of a single IGZO, which implied that oxygen vacancy filaments could be easily ruptured due to the higher oxygen vacancy peak in the HRS layer. The linearity and symmetric of LTP and LTD characteristics for the bi-layer IGZO/ZnO memristor improved a lot compared to a single IGZO memristor. Therefore, the role of the ZnO layer in the bi-layer IGZO/ZnO memristor was potentially significant and essential for charge carriers to be injected easily under a small set voltage and a reset voltage, and the switching behavior to form the conductive path.

Declarations

Data availability

The datasets generated during and/or analyzed during the current study are available from the corresponding author on reasonable request.

Additional Information

Competing Interests: The authors declare that they have no competing interests.

Acknowledgements

This work was supported by the National Research Foundation of Korea (NRF) grant funded by the Korean government (MSIT) (NRF-2019M3F3A1A01074449).

This work was also supported in part by the Ministry of Education of the Republic of Korea and the National Research Foundation of Korea (NRF2019S1A5C2A03081332).

Author Contributions

H.W. Choi conducted most of the experiments and wrote the manuscript including preparing figures and electrical characterization; H.W Choi, K.W. Song, S.H Kim, and K.T Nguyen prepared the original draft of the manuscript. H.M. Kwon and H.D. Lee initiated the work, provided the main idea, supervised the entire process, and reviewed the manuscript; all authors analyzed and discussed the results. All authors have read and agreed to the published version of the manuscript. Funding acquisition was supported by H.D Lee.

References

1. Hebb, D. O. *The Organization of Behavior: A Neuropsychological Theory* (Psychology Press, 2005)
2. Gerstner, W., Ritz, R. & van Hemmen, J. L. Why spikes? Hebbian learning and retrieval of time-resolved excitation patterns. *Biol. Cybern.*69, 503–515 (1993). 10.1007/BF00199450, 7903867
3. Indiveri, G., Chicca, E. & Douglas, R. A VLSI array of low-power spiking neurons and bistable synapses with spike-timing dependent plasticity. *IEEE Trans. Neural Netw.*17, 211–221 (2006). 10.1109/TNN.2005.860850, 16526488
4. Hahnloser, R. H., Sarpeshkar, R., Mahowald, M. A., Douglas, R. J. & Seung, H. S. Digital selection and analogue amplification coexist in a cortex-inspired silicon circuit. *Nature*405, 947–951 (2000). 10.1038/35016072, 10879535
5. Diorio, C., Hasler, P., Minch, A. & Mead, C. A. A single-transistor silicon synapse. *IEEE Trans. Electron Devices*43, 1972–1980 (1996). 10.1109/16.543035
6. Yakopcic, C., Taha, T. M., Subramanyam, G., Pino, R. E. & Rogers, S. A memristor device model. *IEEE Electron Device Lett.*32, 1436–1438 (2011). 10.1109/LED.2011.2163292
7. Lanza, M., et al. Recommended methods to study resistive switching devices. *Adv. Electron. Mater.* 5 (2019). 10.1002/aelm.201800143, 1800143
8. Beck, A., Bednorz, J. G., Gerber, C., Rossel, C. & Widmer, D. Reproducible switching effect in thin oxide films for memory applications. *Appl. Phys. Lett.*77, 139–141 (2000). 10.1063/1.126902
9. Liu, Sd. Q., Wu, N. J. &Ignatiev, A. Electric-pulse-induced reversible resistance change effect in magnetoresistive films. *Appl. Phys. Lett.* 76, 2749–2751 (2000). 10.1063/1.126464

10. Kim, S. G., Han, J. S., Kim, H., Kim, S. Y. & Jang, H. W. Recent advances in memristive materials for artificial synapses. *Adv. Mater. Technol.*3 (2018). 10.1002/admt.201800457, 1800457
11. Mohammad, B. et al. State of the art of metal oxide memristor devices. *Nanotechnol. Rev.*5, 311–329 (2016). 10.1515/ntrev-2015-0029
12. Burr, G. W., et al. Neuromorphic computing using non-volatile memory. *Adv. Phys.* X2, 89–124 (2017). 10.1080/23746149.2016.1259585
13. Waser, R. &Aono, M. Nanoionics-based resistive switching memories. *Nat. Mater.* 6, 833–840 (2007). 10.1038/nmat2023. 17972938
14. Yoshida, C., Tsunoda, K., Noshiro, H. & Sugiyama, Y. High speed resistive switching in Pt/ Ti O 2/ Ti N film for nonvolatile memory application. *Appl. Phys. Lett.*91 (2007). 10.1063/1.2818691, 223510
15. Syu, Y.-E., et al. Atomic-level quantized reaction of HfOx memristor. *Appl. Phys. Lett.*102 (2013). 10.1063/1.4802821, 172903
16. Wang, H., et al. Bio-inspired synthesis of mesoporous HfO 2 nanoframes as reactors for piezotronic polymerization and Suzuki coupling reactions. *Nanoscale*11, 5240–5246 (2019). 10.1039/c9nr00707e, 30864599
17. Kim, S., et al. Experimental demonstration of a second-order memristor and its ability to biorealistically implement synaptic plasticity. *Nano Lett.*15, 2203–2211 (2015). 10.1021/acs.nanolett.5b00697, 25710872
18. Li, X., et al. Electrode-induced digital-to-analog resistive switching in TaO x-based RRAM devices. *Nanotechnology*27 (2016). 10.1088/0957-4484/27/30/305201, 305201
19. Seo, K., et al. Analog memory and spike-timing-dependent plasticity characteristics of a nanoscale titanium oxide bilayer resistive switching device. *Nanotechnology*22, 254023 (2011). 10.1088/0957-4484/22/25/254023
20. Gao, L., et al. Fully parallel write/read in resistive synaptic array for accelerating on-chip learning. *Nanotechnology*26, 455204 (2015). 10.1088/0957-4484/26/45/455204
21. Park, J., et al. TiO x-Based RRAM Synapse With 64-Levels of Conductance and Symmetric Conductance Change by Adopting a Hybrid Pulse Scheme for Neuromorphic Computing. *IEEE Electron Device Lett.* 37, 1559–1562 (2016). 10.1109/LED.2016.2622716
22. Fan, Y.-S., Liu, P.-T. & Hsu, C.-H. Investigation on amorphous InGaZnO based resistive switching memory with low-power, high-speed, high reliability. *Thin Solid Films*549, 54–58 (2013). 10.1016/j.tsf.2013.09.033
23. Chen, M.-C., et al. Influence of electrode material on the resistive memory switching property of indium gallium zinc oxide thin films. *Appl. Phys. Lett.*96 (2010). 10.1063/1.3456379, 262110
24. Kimizuka, N. & Yamazaki, S. *Physics and Technology of Crystalline Oxide Semiconductor CAAC-IGZO: Fundamentals* (John Wiley & Sons, 2016)
25. Kim, M.-S., et al. Effects of the oxygen vacancy concentration in InGaZnO-based resistance random access memory. *Appl. Phys. Lett.*101 (2012). 10.1063/1.4770073, 243503

26. Kim, S., et al. Engineering synaptic characteristics of TaOx/HfO2 bi-layered resistive switching device. *Nanotechnology*29, 415204 (2018). 10.1088/1361-6528/aad64c
27. Wang, J.,Zhuge, X. &Zhuge, F. Hybrid oxide brain-inspired neuromorphic devices for hardware implementation of artificial intelligence. *Sci. Technol. Adv. Mater.* 22, 326–344 (2021). 10.1080/14686996.2021.1911277, 34025215
28. Li, J., et al. Tuning analog resistive switching and plasticity in bilayer transition metal oxide based memristive synapses. *RSC Adv.*7, 43132–43140 (2017). 10.1039/C7RA07522G
29. Park, S., et al. Neuromorphic speech systems using advanced ReRAM-based synapse.*IEEE International Electron Devices Meeting* (IEEE, 2013)
30. Romero, L. P., et al. Training fully connected networks with resistive memories: impact of device failures. *Faraday Discuss.*213, 371–391 (2019). 10.1039/c8fd00107c, 30357183
31. Thakur, C. S., et al. Large-scale neuromorphic spiking array processors: A quest to mimic the brain. *Front. Neurosci.*12, 891 (2018). 10.3389/fnins.2018.00891, 30559644
32. Yu, S., et al. Scaling-up resistive synaptic arrays for neuro-inspired architecture: challenges and prospect.*IEEE International Electron Devices Meeting (IEDM)* (IEEE, 2015)
33. Lim, E. W. & Ismail, R. Conduction mechanism of valence change resistive switching memory: a survey. *Electronics*4, 586–613 (2015). 10.3390/electronics4030586
34. Mondal, S.,Chueh, C.-H. & Pan, T.-M. Current conduction and resistive switching characteristics of Sm2O3 and Lu2O3 thin films for low-power flexible memory applications. *J. Appl. Phys.*115, 014501 (2014). 10.1063/1.4858417
35. Yu, L.-E., et al. Structure effects on resistive switching al/TiOx/al devices for RRAM applications. *IEEE Electron Dev. Lett.*29, 331–333 (2008)
36. Liu, Q., et al. Resistive switching memory effect of ZrO[sub 2] films with Zr[sup +] implanted. *Appl. Phys. Lett.*92, 012117 (2008). 10.1063/1.2832660
37. Peng, H. & Wu, T. Nonvolatile resistive switching in spinel ZnMn 2 O 4 and ilmenite ZnMnO 3. *Appl. Phys. Lett.*95 (2009). 10.1063/1.3249630, 152106
38. Lee, H. Y., et al. Low-power and nanosecond switching in robust hafnium oxide resistive memory with a thin Ti cap. *IEEE Electron Device Lett.*31, 44–46 (2009). 10.1109/LED.2009.2034670
39. Chen, C., Yang, Y. C., Zeng, F. & Pan, F. Bipolar resistive switching in Cu/AlN/Pt nonvolatile memory device. *Appl. Phys. Lett.*97 (2010). 10.1063/1.3483158, 083502
40. Ismail, M., et al. Forming-free bipolar resistive switching in nonstoichiometric ceria films. *Nanoscale Res. Lett.*9, 45 (2014). 10.1186/1556-276X-9-45, 24467984
41. Wang, I., et al. 3D Ta/TaO x/TiO2/Ti synaptic array and linearity tuning of weight update for hardware neural network applications. *Nanotechnology*27 (2016). 365204
42. Bae, J.-H., Lim, S., Park, B. & Lee, J. High-density and near-linear synaptic device based on a reconfigurable gated Schottky diode. *IEEE Electron Device Lett.*38, 1153–1156 (2017). 10.1109/LED.2017.2713460

Figures

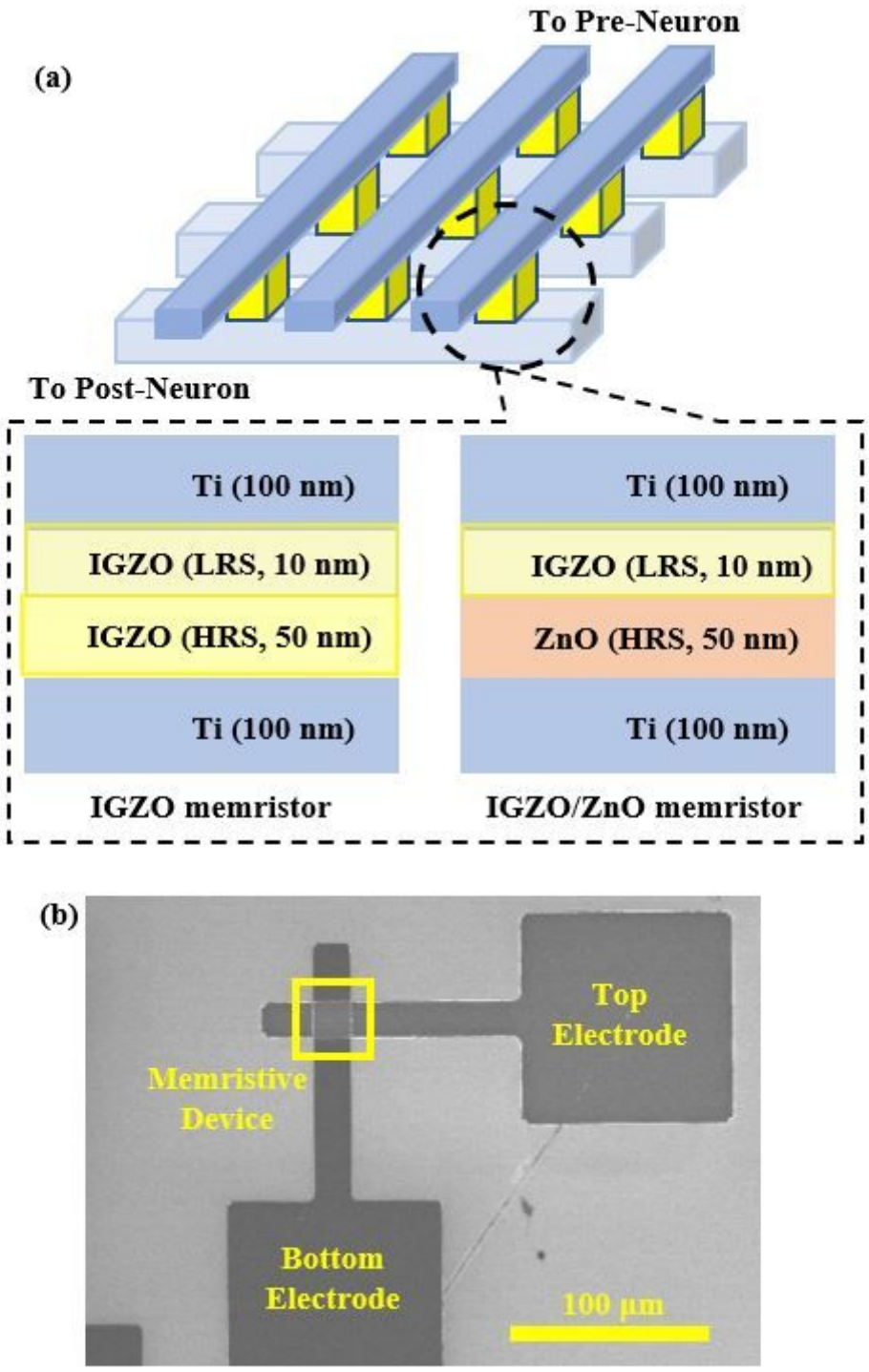

Figure 1

(a) Top image of a crossbar array memristors integrated on a CMOS wafer, (b) TEM image of a memristor and integrated circuit, and (c) a schematic diagram highlighting the vertical integration of the crossbar array with CMOSFETs

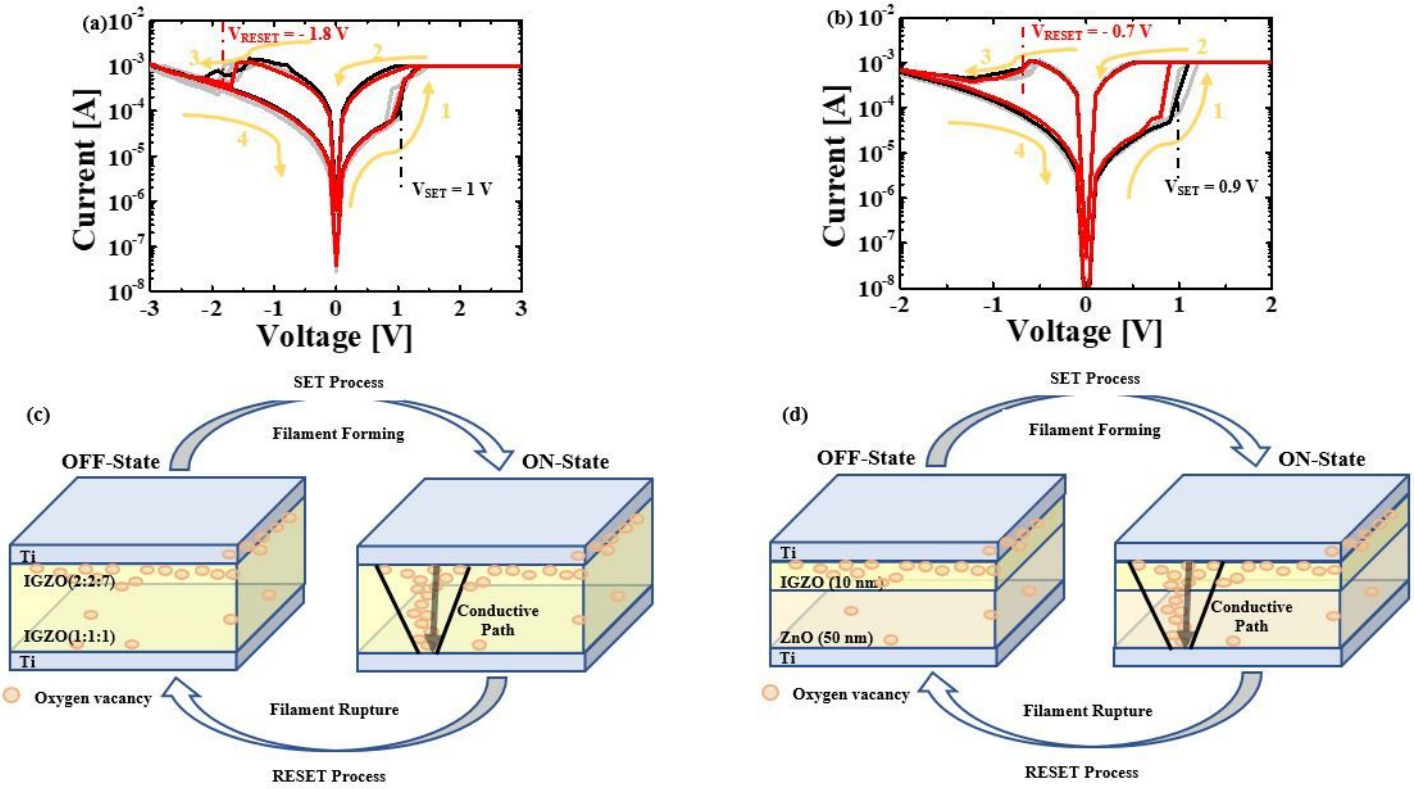

Figure 2

I-V typical bipolar switching behavior of (a) a single IGZO and (b) bi-layer IGZO/ZnO memristors and switching behavior of (c) a single IGZO and (d) bi-layer IGZO/ZnO memristors.

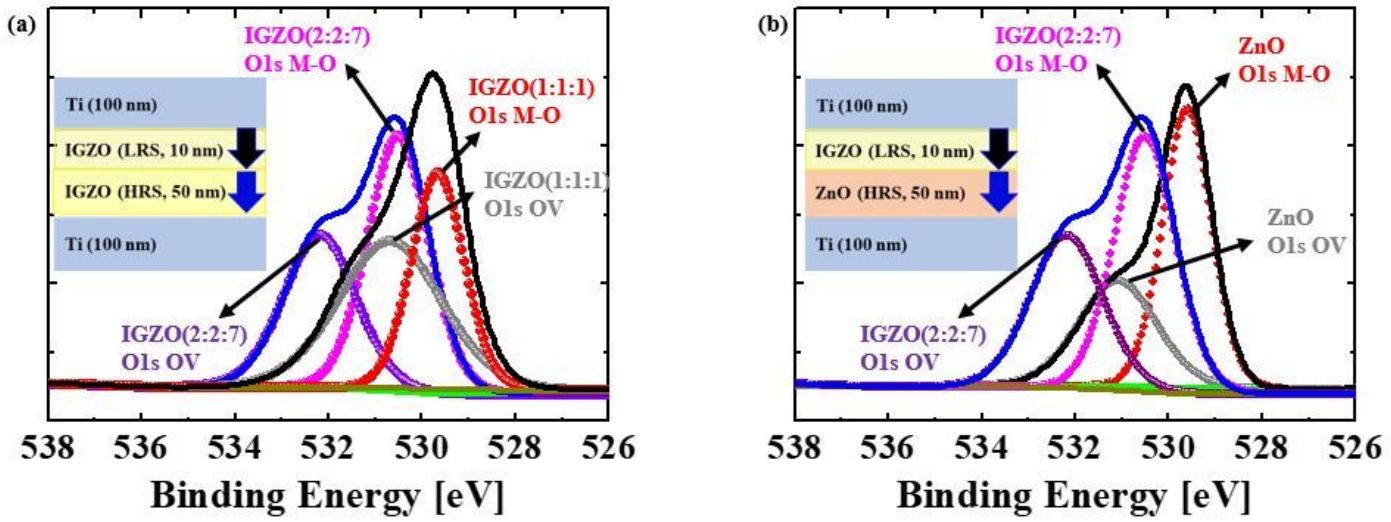

Figure 3

X-ray photoelectron spectroscopy spectra of O1s (a) a single IGZO and (b) bi-layer IGZO/ZnO memristors. The proportions of the oxygen vacancy peaks (O1) of the HRS for a single IGZO and bi-layer IGZO/ZnO

memristors are 45.2% and 38.2%, respectively, while that of LRS for both memristors is about 43.4 %.

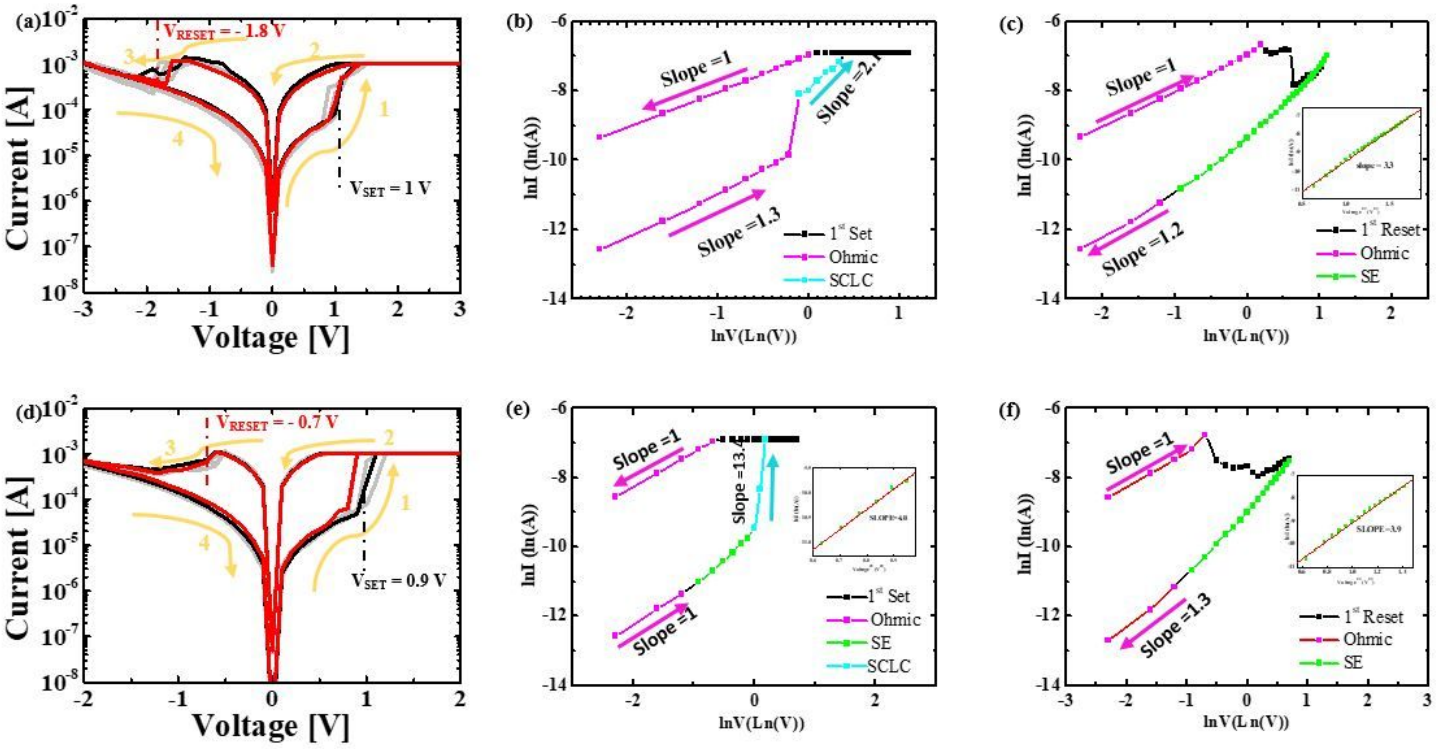

Figure 4

Analysis of conduction mechanism corresponds to SET process and RESET process (a)–(c) a single IGZO memristor and (d)–(f) bi-layer IGZO/ZnO memristor, respectively. Schottky mechanism is observed in a single IGZO and bi-layer IGZO/ZnO memristors at the RESET process, which can be attributed to the interface barrier.

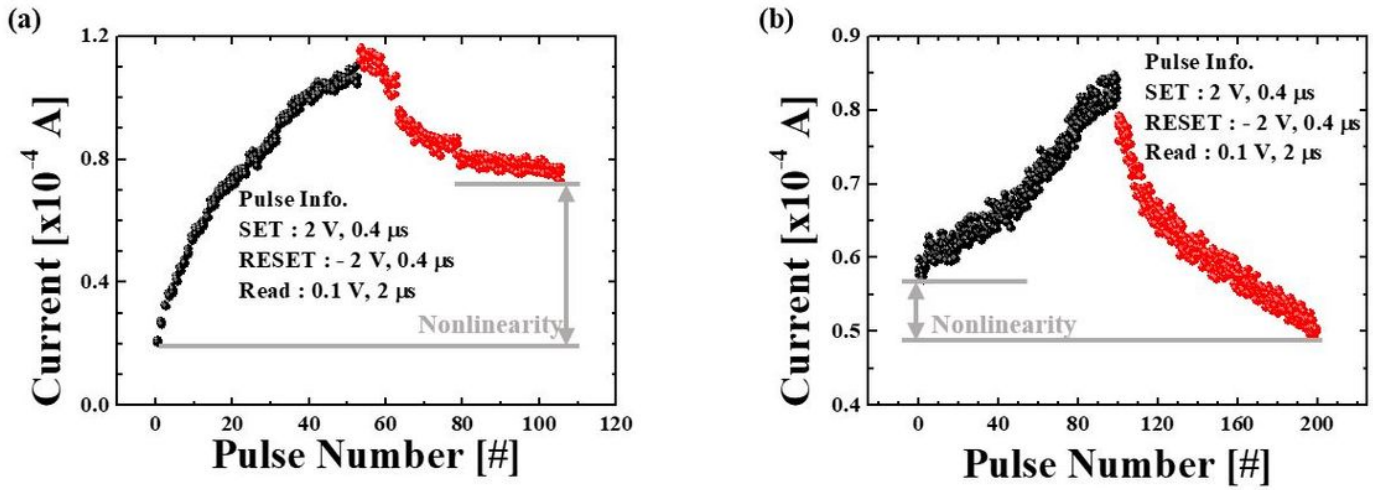

Figure 5

Long-term potentiation and depression characteristics of (a) single IGZO and (b) bi-layer IGZO/ZnO memristors. Applied positive/negative pulses were 50 for a single IGZO and 100 for bi-layer IGZO/ZnO

memristors, respectively, and the current was read after each stimulation pulse was applied. Linearity and symmetricity of LTP and LTD characteristics for bi-layer IGZO/ZnO memristor show more improved linearity than that for a single IGZO memristor.